6th International Conference on Advances in Experimental Structural Engineering
11th International Workshop on Advanced Smart Materials and Smart Structures Technology
August 1-2, 2015, University of Illinois, Urbana-Champaign, United States

Research on the Seismic Performance of an Externally Prestressed Reinforced Concrete Frame

X. Liu [1], L. Lu [2], X.L. Lu[3]

1 *Graduate Student, Research Institute of Structural Engineering and Disaster Reduction, Tongji University, Shanghai, China.*
E-mail: liuxia_tongji@163.com
2 *Associate Professor, Research Institute of Structural Engineering and Disaster Reduction, Tongji University, Shanghai, China.*
E-mail: 95010@tongji.edu.cn
3 *Professor, Research Institute of Structural Engineering and Disaster Reduction, Tongji University, Shanghai, China.*
E-mail: lxlst@tongji.edu.cn

ABSTRACT
In this paper, a new anti-seismic structure (called an Externally Prestressed Rocking Frame, EPRF) is proposed based on previous research, and its seismic performance is validated. First, the theoretical lateral-resistance stiffness formula is provided, and reverse cyclic loading tests of a single-span-single-story EPRF model are presented. Frame stiffness tests are performed under different conditions to obtain hysteresis curves and skeleton curves of the frame. Then, two finite element analytical models are built for comparative analysis: an EPRF with dampers and a conventional frame. Finally, the seismic responses, including the story drifts, floor accelerations and inter-story shear forces, are calculated using the ABAQUS software with time-history dynamic analyses for the ground motion of the El Centro earthquake. The comparative results show that the EPRF with energy-dissipating dampers can greatly reduce the seismic action and also the structural displacement response can be controlled effectively.

KEYWORDS: *external prestressing, rocking frame, time-history analysis, reverse cyclic loading test, seismic performance*

1. INTRODUCTION

The concept of the *Rocking Structure* was proposed by G. W. Housner [1]. Unbonded post-tensioning steel tendons were used in rocking structures by Kurama et al. [2]. Restrepo and Rahman [3] further improved the self-centering walls with hysteretic dampers which are incorporated into these walls to add significant energy dissipation capacity while preserving the self-centering response. Eatherton et al. [4] studied unbounded prestressed tendons placed in controlled rocking of steel-framed buildings with replaceable energy-dissipating fuses. Deierlein et al. [5] proposed a controlled rocking system consisting of three major components: a stiff steel braced frame, vertical post-tensioning tendons and replaceable structural fuses that absorb seismic energy.

Lu et al. [6] presented a new seismic resistance system, the Controlled Rocking Reinforced Concrete Frame (CR-RCF), and performed several experimental studies [7-8] and numerical analyses [9-10]. A shaking table test model and construction details of joints of the CR-RCF are shown in Fig. 1.1.

Then, the authors proposed a new type of anti-seismic structure system called an Externally Prestressed Rocking Frame (EPRF), which is based on the CR-RCF structure. The EPRF structure is shown in Fig. 1.2; the externally prestressed rocking frame includes rocking joints, which significantly reduce the stiffness of the connection by using the pure hinges for the column base and beam-column joints; external prestressing tendons coupled with beams of adjacent floor levels, which generate a prestressing force after post-tensioning and anchoring to the upper and lower beams; and energy-dissipating dampers strategically placed to control the displacement. The steel tendons of the EPRF are in tension using a segment set at an angle between two adjacent beams but not completely in tension from the ends of the foundation to the roof deck, which is a deviation from the rocking wall presented by Kurama et al. [2]. Compared to the CR-RCF structures, the beam-column joint and column base joint are pure hinge joints, so the forces will be more ideal. Furthermore, steel tendons have the advantages of a small prestressing force loss, simple replacement and convenient construction because they are set away from the bodies of the beam and column.

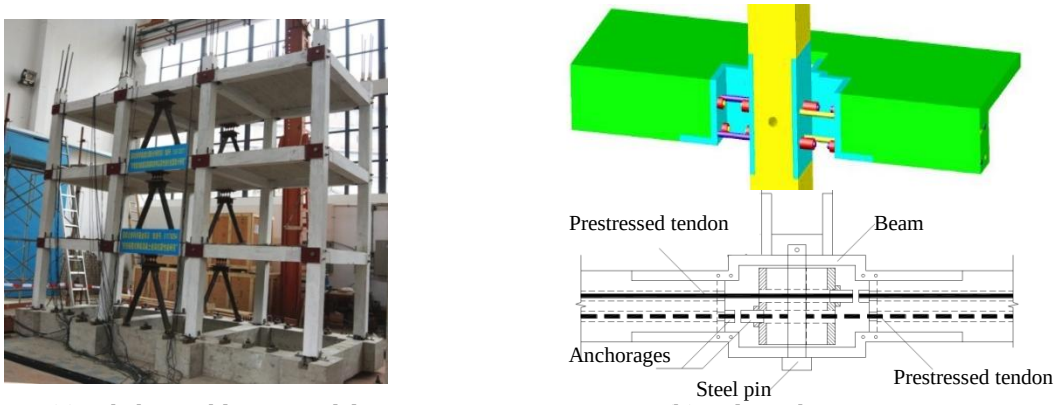

(a) Shaking table test model (b) Column-beam joints

Figure 1.1 Construction details of joints in the CR-RCF

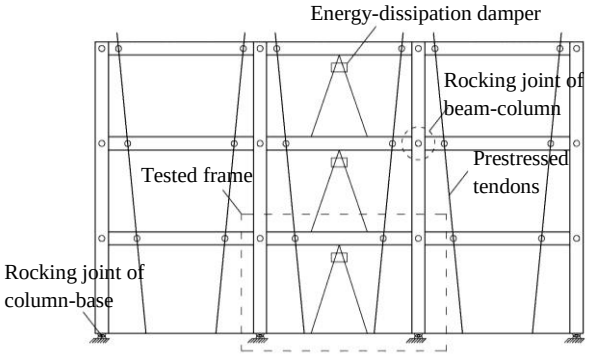

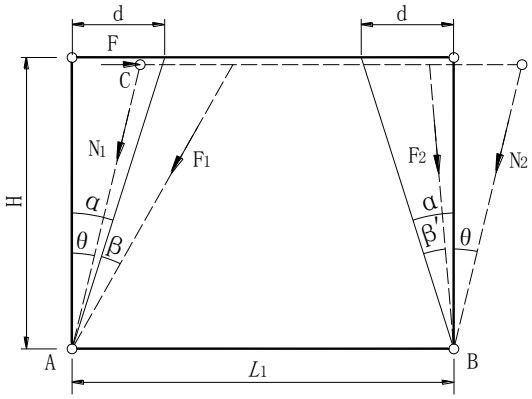

Figure 1.2 Schematic diagram of the EPRF Figure 1.3 Simplified analytical model of the EPRF

The single-span, single-story EPRF model is represented as an analytical model in Fig. 1.3. At any moment during the rocking of the EPRF structures, the frame rotates an angle θ; thus, the dashed line represents the stage of rocking, whereas the solid line represents the initial stage of the EPRF structure, where H=story height; L_1=steel tendons base width; d = relative width between the upper and lower anchorage points; α = prestressing tendons inclination angle, determined as a function of the expected maximum story drift; β and β'= rotation angles of the steel tendons for the left and right sides, respectively, when the frame rotates an angle θ; N_1 and N_2 = the internal forces of the columns for the left and right sides, respectively; and F_1 and F_2= tension forces of prestressing tendons for the left and right sides, respectively. The theoretical overall lateral stiffness formula of the EPRF based on the static balance principle is given by Eq. 1.1.

$$F = \frac{F_1 d\cos(\alpha+\beta) - F_2 d\cos(\alpha-\beta')}{H^2\cos\theta\sin\theta}\cdot\Delta = k_F\Delta \tag{1.1}$$

2. REVERSE CYCLIC LOADING TESTS ON THE EPRF

2.1. Test Profile

The object tested was a single-span, single-story EPRF model. The specimens were constructed on a ½ scale, and the height and span of the model are shown in Fig. 2.1(a). The sizes of cross sections of the beam and column are 150mm×250mm and 250mm×250mm, respectively.

The value of the overall lateral stiffness of the EPRF structures is designed to be 0.206 kN/m, based on the stiffness of the 1/3 scale model of the controlled rocking reinforced concrete frame, CR-RCF [10]. Four standard steel tendons arranged symmetrically have a specification of $\phi^s 15.24$ mm. The ultimate strength, f_{ptk}, is 1860 N/mm^2, and the elastic modulus, E, is 2.0×10^5 MPa. The target design story drift angle, θ_{max}, was chosen to be 5%, based

on the performance criteria and the corresponding target story drift, Δ_y= 90 mm. The value of the inclination angle of the steel tendon, α, in this test was calculated to be 0.069.

The test specimens consisted of a foundation, column base joints, beam-column joints, structural members, steel tendons, damper and braces, as shown in Fig. 2.1. X-type metallic dampers were strategically placed to simulate the energy dissipater. The connections of the beam-column and column base joints are pure hinges, with one side of the steel tendon anchored to the beam and the other side anchored to the rigid foundation.

Reverse cyclic loading was applied in displacement control. A total of 39 cycles of displacement were imposed, consisting of three cycles of lateral displacement of amplitudes of 2, 5, 10, 15, 20, 25, 30, 40, 50, 60, 70, 80, and 90 mm; the last displacement corresponds to a story drift angle of 5%. A schematic diagram of the test model and experimental setup are shown in Fig. 2.1.

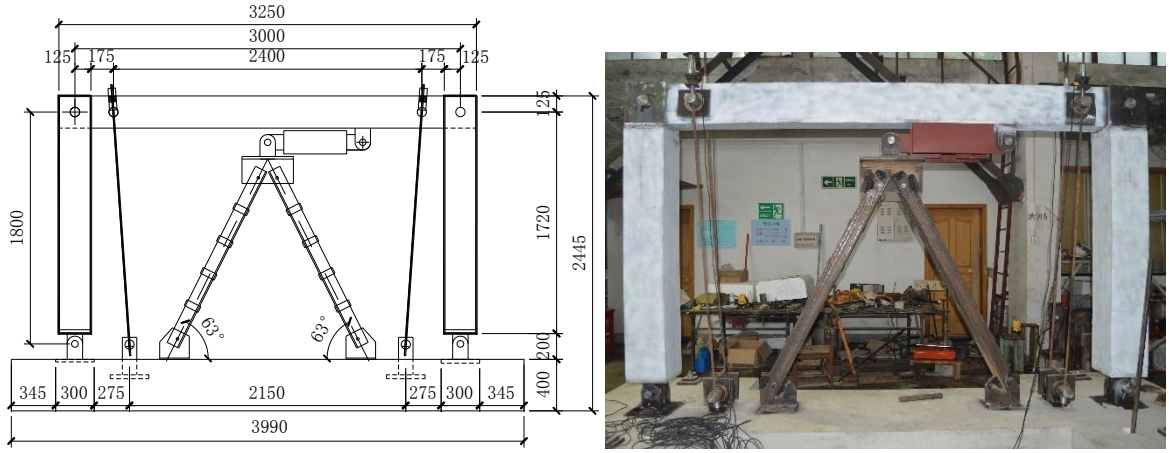

(a) Schematic diagram of the test model (b) Experimental setup

Figure 2.1 Reverse cyclic test of the EPRF

2.2. Experimental Results

Hysteresis curves of an EPRF without a damper and an EPRF with a damper, shown in Fig. 2.2, indicate that the deformation capacity of the EPRF without a damper has a slightly nonlinear behavior and the EPRF with a damper has an excellent energy dissipation capability.

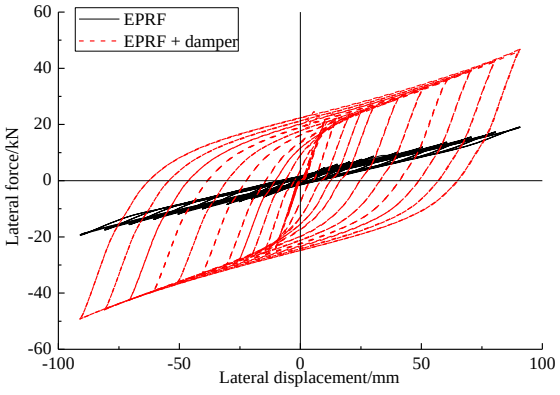

Figure 2.2 Hysteresis curves of the EPRFs

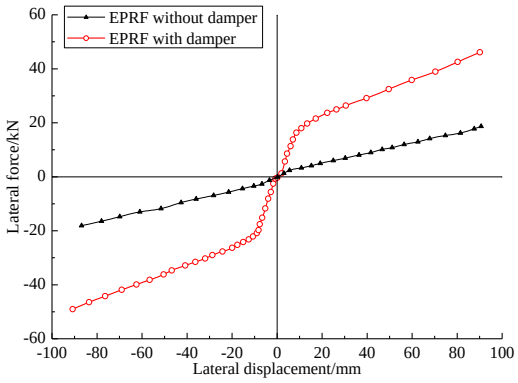

Figure 2.3 Skeleton curves of the EPRFs

The skeleton curves of the rocking frames shown in Fig. 2.3 could be simplified to bilinear curves for both cases with and without dampers. A comparison of the lateral stiffness acquired from the skeleton curves with the theoretical one calculated using Eq. 1.1 is presented; the stiffness of the EPRF acquired from the skeleton curve of the EPRF without a damper is 0.190 kN/m, whereas the theoretical lateral stiffness is 0.206 kN/m. The theoretical lateral stiffness formula agrees well with the test results with an error of 7.8%.

3. NUMERICAL MODELLING METHOD OF THE EPRF

A finite element model was proposed based on the study of the EPRF structure using reverse cyclic loading tests. The finite element program ABAQUS was used to perform the numerical modelling. The column base joint and the beam-column joint are pure hinges. The Axial connection element was adopted to model the spring characteristic of the prestressing tendon. The Cartesian connection element was adopted to model the X-type metallic damper. The beam, column and brace were simulated using the beam element B31.

Because a conventional concrete frame could enter the range of plastic deformation, the reinforced concrete employed the plastic damage model. The constitutive material model of the reinforced concrete is based on a fiber element in ABAQUS and uses a group of uniaxial hysteresis constitutive models called TJ-Fiber [11].

3.1 Numerical simulation of a single-span-single-story EPRF model

The numerical simulations were performed for test cases of the EPRF with a damper. A comparison between the experiment and the numerical simulation is shown in Fig. 3.1. It can be seen that the numerical simulation is consistent with the experiment, which confirms that the numerical modelling method of the EPRF is suitable and effective.

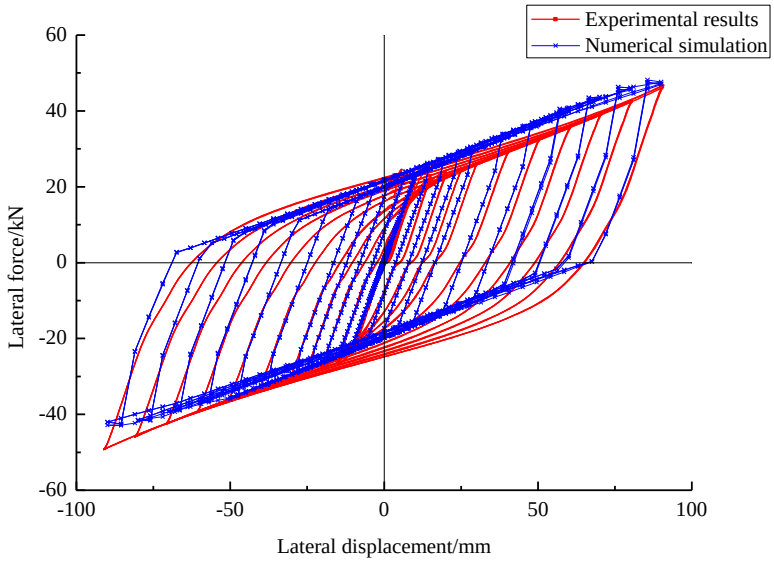

Figure 3.1 Comparison of the experiment and numerical simulation of the EPRF

3.2. Numerical analysis model of the EPRF

The total height of the structure is 10.8 m, with 3.6 m for each story and 6 m for each span in both the transverse (X) and longitudinal (Y) direction, as shown in Fig. 3.2(a). Two frames shown in Fig. 3.2(b) are extracted from the whole structures for analysis. The designated basic acceleration of the ground motion is 0.2 g.

The FEM models of the conventional frame and EPRF with dampers were built. The cross sections of the beams and columns are 300×500 mm and 500×500mm, respectively. The conventional frame is designed to satisfy the seismic requirements stated in the *Code for Seismic Design of Buildings* of China [12]. The representative gravity loads for each floor are 1053kN, 1053kN and 963 kN, respectively.

The target design story drift angle of the whole EPRF structure, θ_{max}, was chosen to be 5%. Then, the inclination angle of steel tendons α, the stiffness of the whole structure and the dampers properties are all referenced to the parameters in the reverse cyclic loading tests of a single-span, single-story EPRF model. As a result, the inclination angle of steel tendons α is 0.069, there are six tendons at each side of each floor, and the specification is $\phi^s 15.24$. Six metallic dampers are set up between the columns of each middle span to control the story drifts of the EPRF. The parameters of the dampers are as follows: initial stiffness is 5.24 kN/mm, yield force is 53.32 kN, and yield

displacement is 10 mm. Referring to the numerical modelling method of the EPRF in the present section, the FEM models of the conventional frame and EPRF with dampers were built, as shown in Fig. 3.3.

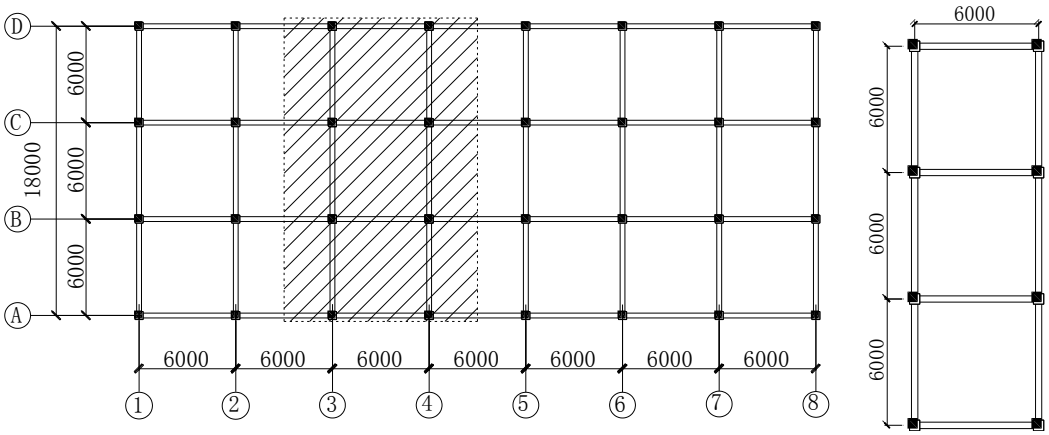

Figure 3.2 Layout of the Frame Structure

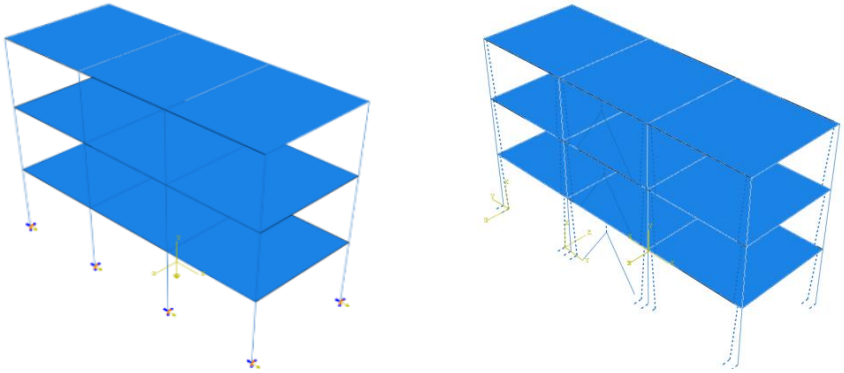

(a) Conventional frame (b) EPRF with dampers

Figure 3.3 FEM models

The fundamental natural periods of the conventional frame and EPRF with dampers in the longitudinal (X) direction obtained from analysis are 0.315 s and 2.618 s, respectively. It is shown that the conventional frame has a shorter period but larger stiffness. On the contrary, the EPRF equipped with dampers strategically results in a decrease of the fundamental natural period and an increase in the stiffness. These results indicate that the lateral stiffness of the EPRF would weaken significantly for rocking joints in the frame. The base shear of the EPRF with dampers, according to the response spectrum theory, decreases when the natural period increases.

4. ANALYSIS OF ANTISEISMIC PERFORMANCE OF THE EPRF

The ground motion selected in this analysis is the commonly used El Centro-EW wave. The El Centro wave is the ground motion record of the Imperial Valley in 1940, which had a maximum acceleration of 341.7 cm/s^2 in the direction of north-south, 210.1 cm/s^2 in the direction of east-west and 206.3 cm/s^2 in the vertical direction.

Numerical analysis of the models of the conventional frame and EPRF with dampers built in Section 3.2 is performed using the El Centro ground motion, which is scaled to a peak ground acceleration (PGA) of 0.07 g, 0.20 g and 0.40 g corresponding to conditions of small, moderate and large earthquakes, respectively. The maximum dynamic responses of the conventional frame and EPRF with dampers are presented in Table 4.1.

Table 4.1 Maximum dynamic responses

	PGA (g)	0.07			0.20			0.40		
Responses	Floor	F1	F2	F3	F1	F2	F3	F1	F2	F3
Displacement	Conventional	2.8	6.0	7.9	9.8	16.9	19.8	18.7	37.6	44.8

(mm)	frame									
	EPRF with dampers	11.7	21.4	29.8	31.9	62.6	95.0	83.5	168.5	255.8
Acceleration (m/s^2)	Conventional frame	1.4	2.5	2.9	3.9	3.9	4.1	6.9	6.8	7.6
	EPRF with dampers	0.9	0.6	0.9	2.5	1.7	2.4	4.6	3.1	4.3
Inter-story shear (kN)	Conventional frame	491.8	371.8	222.8	999.0	712.4	407.6	1400.0	1153	643.2
	EPRF with dampers	200.9	98.1	66.5	421.8	208.8	158.9	757.0	381.8	300.4

The maximum inter-story drifts of the conventional frame and the EPRF with dampers are compared and shown in Fig. 4.1. The EPRF with dampers predict larger inter-story drifts in comparison to the conventional frame for the same intensity of earthquake, which attributes to the excellent deformability of the EPRF. Under a large earthquake, the roof displacement of the EPRF with dampers is 255.8 mm, whereas for the conventional frame this value decreases to 44.8 mm, thus the roof displacement of the conventional frame is approximately 82.5% less than the EPRF with dampers. As seen in Fig. 4.1(c), the maximum inter-story drift of the EPRF with dampers for a large earthquake is 2.4%, which is less than the control target of 5%, indicating the steel tendons are still in the elastic range.

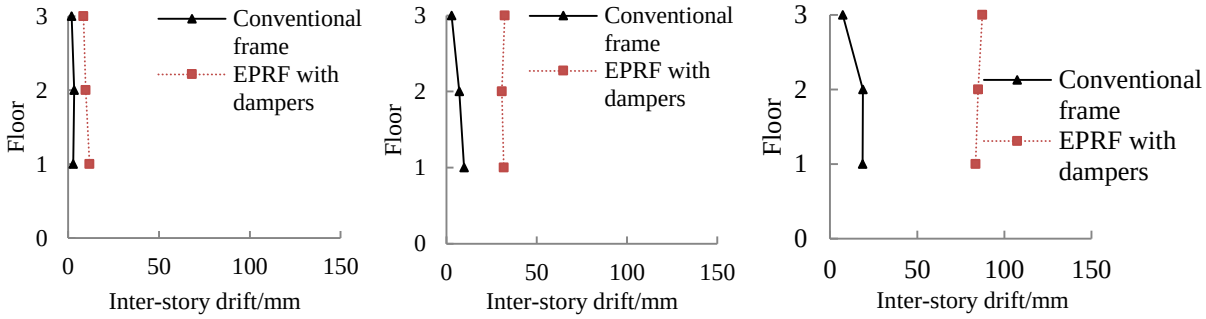

(a) Small earthquake (b) Moderate earthquake (c) Large earthquake

Figure 4.1 Curves of the story drifts

The acceleration response curves of the conventional frame and the EPRF with dampers are displayed in Table 4.2. The results show that the acceleration responses of the EPRF with dampers are less than the conventional frame, which means that the anti-seismic performance of the EPRF is significant.

Table 4.2 Time history curves of the conventional frame and the EPRF with dampers

PGA	Time history curves
0.07 g	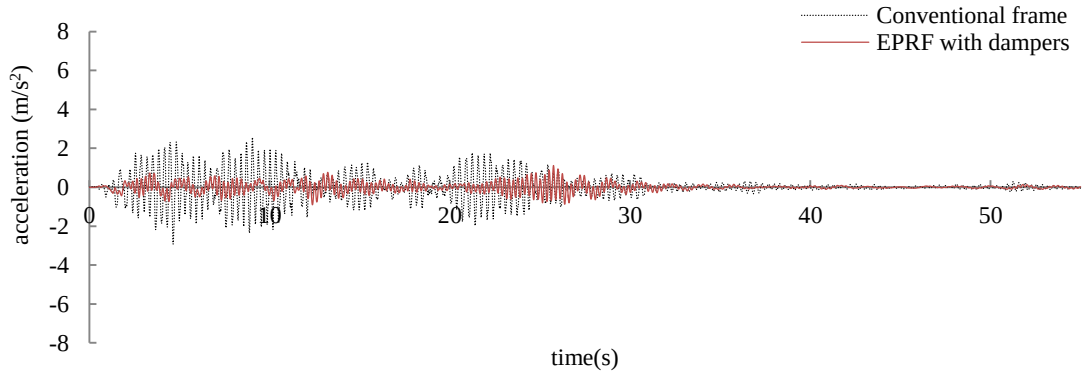

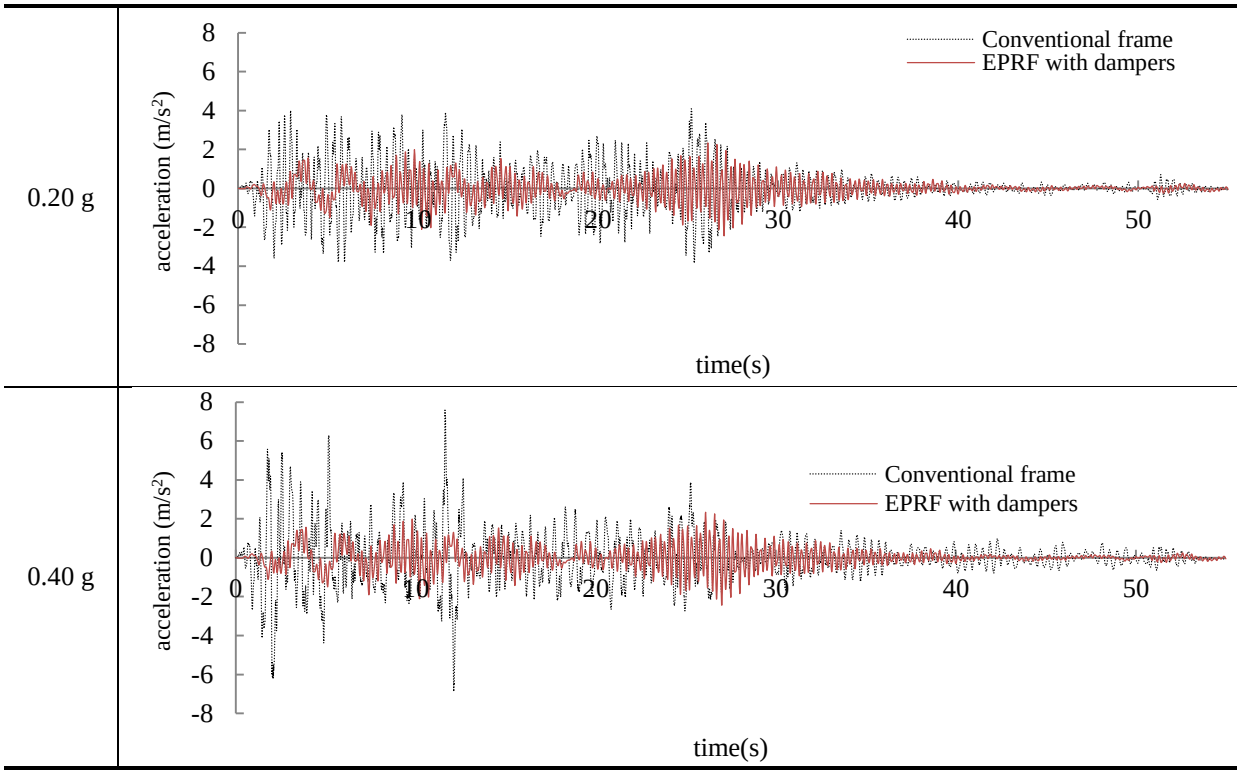

A comparison of inter-story shear force shown in Fig. 4.2 indicates that the EPRF with dampers do necessarily decrease the inter-story shear forces; as the base shear carried by the columns of EPRF with dampers are 59.2%, 57.8% and 45.9% less than those of conventional frame for the conditions of small, moderate and large earthquakes, respectively.

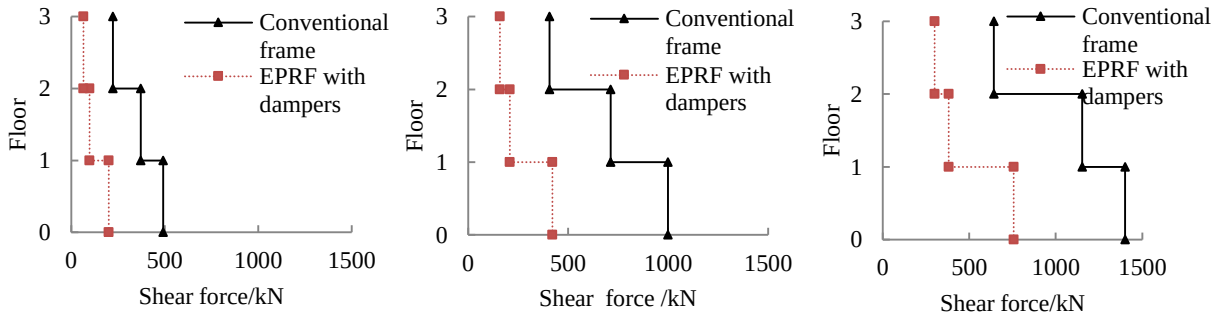

(a) Small earthquake (b) Moderate earthquake (c) Large earthquake

Figure 4.2 Story shear forces

5. CONCLUSIONS

In this paper, a new anti-seismic structure called an Externally Prestressed Rocking Frame (EPRF) is proposed. Reverse cyclic loading tests of a single-span, single-story EPRF model are introduced. Then, two analytical models of the EPRF with dampers and conventional frame are built. Finally, the anti-seismic performances are analyzed by performing a comparison between the story drift, acceleration and inter-story shear force responses. The main conclusions of the study are summarized as follows:

(1) It is evident from the analyses results that the theoretical lateral stiffness formula is sufficiently accurate for the EPRF structure. Based on the reverse cyclic loading tests, it is concluded that the theoretical lateral stiffness formula of the EPRF agrees well with the test results with an error of 7.8%.

(2) It was shown that the lateral stiffness of the EPRF weakens significantly when using the rocking joint, and restoration can be achieved by external prestressing. The EPRF has a larger period than the conventional frame

resulting in a remarkable reduction in the earthquake action on the structure.

ACKNOWLEDGMENT

The authors are grateful for the financial support received from the National Natural Science Foundation of China (grant Nos. 51178354, 51261120377). The materials presented are the research findings of the authors and are not necessarily an expression of the opinion of the funding agency.

REFERENCES

1. Housner, G.W. (1963). The behavior of inverted pendulum structures during earthquakes. *Bulletin of the Seismological Society of America*. **53:2**, 403-417.
2. Kurama, Y., Sause, R., Pessiki, S. et al. (1999). Lateral load behavior and seismic design of unbounded post-tensioned precast concrete walls. *ACI Structural Journal*.**96:4**, 622-632.
3. Restrepo, J. I., Rahman, A. (2007). Seismic performance of self-centering structural walls incorporating energy dissipaters. *Journal of Structural Engineering*. **133:11**, 1560-1570.
4. Eatherton, M., Hajjar, J. F., and Deierlein, G. G. et al. (2008). Controlled Rocking of Steel-Framed Buildings with Replaceable Energy-Dissipating Fuses. *Proceedings of the 14th World Conference on Earthquake Engineering*. Beijing, China.
5. Deierlein, G. G., Hajjar, J. F. and Eatherton, M. et al (2009). Seismically Resilient Steel Braced Frame Systems with Controlled Rocking and Energy Dissipating Fuses. *George E Brown Jr. Network for Earthquake Engineering Simulation (NEES) 7th Annual Meeting*. Honolulu, USA.
6. Lu, L., Lu, X. L., and Zhu, F. B., et al (2013). Experimental Study on Seismic Performance of a Controllable Rocking Reinforced Concrete Frame. *Proceedings of the Fifth International Conference on Advances in Experimental Structural Engineering.* Taipei, China.
7. Lu, L., Fan, Y., and Liu L., et al (2015). Research on the seismic performance of controlled rocking RC frame. *Journal of earthquake engineering and engineering dynamics.***34:1**, 66-76. (in Chinese)
8. Lu, L., Liu, X., and Chen, J. J. et al. (2015). Seismic Performance Study on a Rocking Reinforced Concrete Frame with Push-over Analysis. *Journal of earthquake engineering and engineering dynamics.***35:2**, 124-131. (in Chinese)
9. Lu, L., Chen, J. J. and Lu, X. L. (2014). Numerical Analysis of the Seismic Performance of a Controllable Rocking Reinforced Concrete Frame. *Proceedings of the 13th International Symposium on Structural Engineering.* Hefei, China.
10. Lu, L., Liu, X., and Chen, J. J. et al. (2015). Parameter Research of Joints Stiffness in a Rocking Reinforced Concrete Frame. *Journal of Vibration and Shock.***34:13**, 195-199. (in Chinese)
11. Wu, X. H. (2008). Manual of Transformation from NosaCAD to ABAQUS model [EB/OL]. *http://www.nosacad.com/xzzx.htm*.
12. National Standards of the People's Republic of China. GB50011-2010 (2010). Code for seismic design of buildings. *China Architecture Industry Press*, Beijing, China. (in Chinese)